J Korean Soc Appl Biol Chem (2015) 58(3):433–442
DOI 10.1007/s13765-015-0038-6

Online ISSN 2234-344X
Print ISSN 1738-2203

ARTICLE

Different shapes of Al_2O_3 particles induce differential cytotoxicity via a mechanism involving lysosomal destabilization and reactive oxygen species generation

Byung Il Kim · Yong Hoon Joo · Pyo June Pak · Joong-Su Kim · Namhyun Chung

Received: 15 December 2014 / Accepted: 23 December 2014 / Published online: 24 March 2015

Abstract The biological effects of nano- and micro-sized Al_2O_3 particles are hypothesized to differ according to the shapes as well as the sizes of the particles. Thus, the mechanisms of interleukin (IL)-1β production and the association between the shape of the Al_2O_3 particle and its cytotoxicity in macrophage-like THP-1 cells were investigated using particles with three different shapes [N-Al_2O_3 (<30 nm), S-Al_2O_3 (2–4 nm × 100–800 nm), L-Al_2O_3 (2–4 nm × 2800 nm)]. Levels of IL-1β production and cytotoxicity were concentration-dependent and were in the following order: S-Al_2O_3 > N-Al_2O_3 > L-Al_2O_3. Stimulus of THP-1 cells by Al_2O_3 particles led to lysosomal destabilization, generation of intracellular reactive oxygen species (ROS), and subsequent release of cathepsin B. The magnitude of the stimulus was dependent on the shapes and aspect ratios of the particles. Additional results suggested that caspase-1 (NALP3 inflammasome) activation and IL-1β production followed cathepsin B release. In addition, the cell death induced by Al_2O_3 particles was closely related with cathepsin B leakage. The mode of cell death was necrotic as much as apoptotic. We conclude that Al_2O_3 particles induce different levels of IL-1β production and cytotoxicity depending on their particle shapes or aspect ratios. The current finding may support the development of safe forms of Al_2O_3 particles.

Keywords Cytotoxicity · Interleukin-1beta · Lysosomal destabilization · Cathepsin B · Reactive oxygen species

Introduction

With the rapid development of nanotechnology and its applications, a wide variety of nanomaterials (NMs), less than 100 nm in at least one dimension, are now used in a variety of industrial fields. Fiber-shaped NMs such as nanowires and nanotubes have also been designed for use in biomedical applications (Roy et al. 2012). These fiber-shaped NMs have great benefit in diverse fields due to their unique structures (Li et al. 2012). Nowadays, metal oxide NMs such as aluminum oxide (Al_2O_3), titanium oxide (TiO_2), iron oxide (Fe_2O_3, Fe_3O_4), and zinc oxide (ZnO) are the most commonly used oxides in diverse fields. Al_2O_3 nanoparticles (NPs) are some of the most frequently manufactured NPs (Piccinno et al. 2012). However, the increasing popularity of Al_2O_3 NP applications has raised public concern about their safety. Al_2O_3 is relatively more stable than aluminum and can easily enter the body via inhalation, skin contact, and food ingestion. Recently, a number of studies have demonstrated that Al_2O_3 NPs exert cytotoxic effects and are able to cause genotoxicity in vivo and in vitro (Kim et al. 2009; Morsy et al. 2013). Furthermore, Al_2O_3 NPs were found to induce the production of pro-inflammatory cytokines such as interleukin-1β (IL-1β) in macrophages (Yagil-Kelmer et al. 2004). Thus, there

Byung Il Kim, Yong Hoon Joo, and Pyo June Pak have contributed equally to this study.

Electronic supplementary material The online version of this article (doi:10.1007/s13765-015-0038-6) contains supplementary material, which is available to authorized users.

B. I. Kim · Y. H. Joo · P. J. Pak · J.-S. Kim · N. Chung (✉)
College of Life Sciences and Biotechnology, Korea University, Seoul 136-712, Republic of Korea
e-mail: nchung@korea.ac.kr

J.-S. Kim (✉)
Jeonbuk Branch Institute, Korea Research Institute of Bioscience and Biotechnology, Jeongeup 580-185, Republic of Korea
e-mail: joongsu@kribb.re.kr

is a need to investigate the mechanisms of Al_2O_3 -induced inflammatory responses and biological effects according to the particle characteristics including size and shape (i.e., nanospheres vs. nanowires).

Inflammation is part of the complex biological response of vascular tissues to harmful stimuli such as pathogens and irritants that occur during infections or after tissue damage (Stutz et al. 2009). Immune system cells such as macrophages play a crucial role in inflammatory responses and can produce cell-derived mediators including cytokines. Among them, IL-1β is a prominent and early cytokine that exerts various effects on the immune system. IL-1β is initially produced in the cytosol as an inactive precursor to pro-IL-1β and is later converted to mature IL-1β by caspase-1, which is in turn activated by a large multimolecular complex known as NACHT, LRR, and PYD domains-containing protein 3 (NALP3) inflammasome (Burns et al. 2003; Agostini et al. 2004). Pathogen-associated molecular patterns (PAMPs) and damage-associated molecular patterns (DAMPs) trigger the assembly of inflammasomes (Allen et al. 2009; Tschopp and Schroder 2010). Activated NALP3 inflammasomes interact with apoptosis-associated speck-like protein containing a C-terminal caspase-recruitment domain which recruits pro-caspase-1 (Halle et al. 2008).

Though the detailed mechanisms of NALP3 inflammasome activation remain unclear, one group's report showed that silica crystals and aluminum salts can activate NALP3 inflammasomes through phagosomal destabilization (Hornung et al. 2008). However, it is uncertain whether IL-1β production induced by Al_2O_3 particles is similarly dependent on the activation of NALP3 inflammasomes and whether different shapes or forms of Al_2O_3 particles induce IL-1β production via common or distinct intracellular pathways. Thus, in the present study, we aim to elucidate the associations between different shapes of Al_2O_3 particles and IL-1β production in macrophage-like THP-1 cells. We also aim to correlate IL-1β production mechanism with the cytotoxcity induced by Al_2O_3 particles of different shapes.

Materials and methods

Chemicals

RPMI 1640, penicillin, streptomycin, and fetal bovine serum (FBS) for cell culture were purchased from WelGENE Inc. (Korea). PreMix WST-1 Cell Proliferation Assay System and Lactate dehydrogenase (LDH) Cytotoxicity Detection Kit for measurement of cytotoxicity of Al_2O_3 particles were purchased from TakaRa Bio Inc. (Japan). Propylene oxide and EPON epoxy resin to observe the image of transmission electron microscopy (TEM) were purchased from Acros Organics (USA) and Electron Microscopy (USA), respectively. CA-074-methyl ester (CA-074-Me), diphenyleneiodonium chloride (DPI), butylated hydroxyanisole (BHA), 2′,7′-difluorescencein diacetate (DCFH-DA), and phorbol 12-myristate 13-acetate (PMA) were obtained from Sigma-Aldrich (USA). Z-WEHD-FMK for caspage-1 specific inhibition and IL-1β Enzyme-linked immunosorbent assay (ELISA) kit were purchased from R&D Systems (USA). Apoptosis Detection kit was purchased from BD Biosciences (USA).

Treatment of Al_2O_3 particles

The cells were seeded 5×10^5 cells/mL in 6-well plates, received 0.5 μM PMA for differentiation into macrophage-like cell, and incubated overnight. All particles were suspended in serum-free RPMI 1640 to make stock solutions (2 mg/mL) prior to each experiment. The stock solution was sonicated for 3 min to disperse the particles, and diluted to working concentrations (25, 50, 100, and 200 μg/mL). Then, cell medium was replaced with serum-free PRMI 1640 containing nano-sized Al_2O_3 (N-Al_2O_3; <50 nm; Sigma-Aldrich) and long-Al_2O_3 (L-Al_2O_3; 2–4 nm × 2,800 nm; Sigma-Aldrich), and short-Al_2O_3 (S-Al_2O_3; 2–4 nm × 100–800 nm; Nano Technology Inc., Korea).

Cell culture

Human acute monocytic leukemia cell line (THP-1; KCLB #. 40202) were obtained from Korean Cell Line Bank (KCLB; Korea). The cells were grown in RPMI 1640 medium supplemented with 10 % heat-inactivated FBS, 100 U/ml penicillin, 100 μg/mL streptomycin, and 0.05 mM β-mercaptoethanol. The cells were maintained at 37 °C in a 5 % CO_2 incubator.

WST-1 cytotoxicity assay

THP-1 cells were seeded at 96-well plates. After differentiation into macrophages, various concentrations of Al_2O_3 particles were added to the PMA-primed cell for 24 h. Cell viability was determined using a PreMix WST-1 Cell Proliferation Assay System according to the manufacturer's protocol. Briefly, 10 μL of WST-1 reagent was added each well, and the plates were incubated for 2 h. The absorbance of WST-1-containing samples was quantified at 490 nm by a microplate reader (EL800, Bio-Tek, USA).

LDH release assay

PMA-primed THP-1 cells were prepared as described in the WST-1 cytotoxicity assay section, and treated with the

particles for 24 h. Supernatant of the particle-treated cells was obtained by centrifugation and analyzed the LDH Cytotoxicity Detection Kit according to the manufacturer's protocol.

TEM analysis

Phagocytosis of Al_2O_3 particles was observed using TEM (JEM-7401F, JEOL, Japan). Briefly, 50 μg/mL of Al_2O_3 particles were exposed to PMA-primed THP-1 cells for 6 h and gently washed with phosphate-buffered saline twice. The particle-treated cells were fixed overnight in 2.5 % glutaraldehyde. Post-fixation staining was done using 2 % osmium tetroxide for 1.5 h. The samples were then washed well with deuterated H_2O, dehydrated by a graded series of ethanol, infiltrated using propylene oxide, mixed with EPON epoxy resin, and finally embedded with only epoxy resin. Appropriate areas for thin sectioning were cut at 65 nm. Then, the section was stained with saturated 4 % uranyl acetate and 4 % lead citrate before examination at 80 kv.

ELISA

PMA-primed THP-1 cells were exposed to various concentrations of Al_2O_3 particles for 6 h. Levels of IL-1β production in the supernatant of cell culture were analyzed using an ELISA kit according to the manufacturer's protocol. For inhibitor effect assays, the cells were pre-incubated with RPMI 1640 containing cytochalasin D, CA-074-Me, DPI, BHA, or Z-WEHD-FMK for 30 min in 6-well culture plate prior to treatments of Al_2O_3 particles.

Acridine orange staining

Lysosomal membrane permeabilization was observed using acridine orange staining of lysosome (Boya et al. 2003). PMA-primed THP-1 cells were treated with 0.5 μg/mL acridine orange in RPMI 1640 for 30 min. After staining solution treatment, the cells were washed with RPMI 1640 at three times and treated with various concentrations of Al_2O_3 particles for 6 h. The fluorescence intensity at excitation/emission wavelengths of 488/620 nm was assessed using FACSCalibur (BD Biosciences).

Measurement of reactive oxygen species (ROS) production

For measurement of the extent of intracellular ROS, PMA-primed THP-1 cells were treated with various concentrations of Al_2O_3 particles and were loaded with 20 μM DCFH-DA in 6-well plates for 45 min (Hiura et al. 1999; Arrigo et al. 2005). The fluorescence intensity was promptly measured with FACSCalibur at an excitation/emission wavelength of 488/530 nm.

Annexin V-FITC/propidium iodine (PI) staining

Apoptotic and necrotic cells were analyzed by flow cytometry with the Apoptosis Detection Kit. PMA-primed THP-1 cells were exposed with various concentrations of Al_2O_3 particles. The cells were harvested after 6 h by centrifugation, were then resuspended in Annexin V binding buffer. The cells were loaded with 5 μL of Annexin V-FITC and PI solution, respectively. The cell suspension was incubated in the dark for 15 min at room temperature. The fluorescence intensities of Annexin V-FITC and PI were measured with FACSCalibur at excitation/emission wavelengths of 488/530 and 488/617 nm, respectively.

Results

Cytotoxicity of Al_2O_3 particles

To assess the cytotoxicity of Al_2O_3 particles, the cell viability of PMA-primed THP-1 cell lines was analyzed by WST-1 assay. The results showed that the degree of cytotoxicity was shape- and concentration-dependent (Fig. 1a). Especially, both N-Al_2O_3 and S-Al_2O_3 significantly decreased the viability of PMA-primed THP-1 cells. Even very low concentrations of either compound (25 μg/mL) caused the cell viability to decrease. The viability of cells treated with 200 μg/mL of S-Al_2O_3 was only 22.9 %. and the overall degree of cytotoxicity with Al_2O_3 particles was in the order of S-Al_2O_3 > N-Al_2O_3 > L-Al_2O_3.

To assess the cell membrane damage caused by Al_2O_3 particles, the release of LDH in culture medium was measured (Fig. 1b). When PMA-primed THP-1 cells were incubated in the presence of L-Al_2O_3, almost no change in LDH release was observed. However, when the cells were exposed to N- and S-Al_2O_3, significantly increased LDH release (i.e., about 300 and 270 % increase for N-Al_2O_3 and S-Al_2O_3 at 100 μg/mL, respectively) was observed. This result suggests that membrane integrity is disrupted more strongly by N- and S-Al_2O_3 than L-Al_2O_3.

Influence of Al_2O_3 particles on IL-1β production

To evaluate the correlation between particle shape and inflammatory effect of Al_2O_3 particles, the levels of IL-1β production in PMA-primed THP-1 cells were investigated in the presence of various Al_2O_3 particles. THP-1 cells were incubated for 6 h with each kind of Al_2O_3 particle at concentrations ranging from 0 to 200 μg/mL. At all of the concentrations tested, both N-Al_2O_3 and S-Al_2O_3 induced

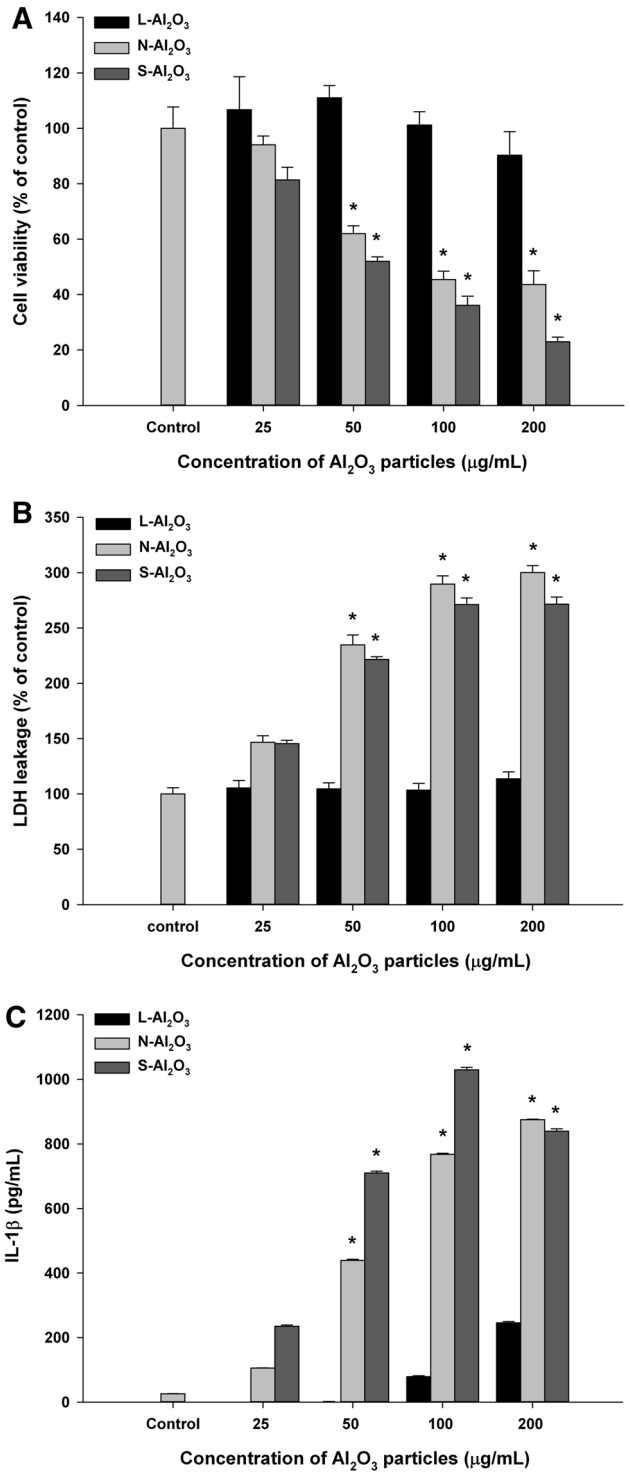

◀**Fig. 1** Effect of the shape of Al_2O_3 particles on cytotoxicity and interleukin-1 β production. **a** Cell viability was measured by WST-1 assay. **b** LDH leakage due to membrane damage was measured using a LDH Cytotoxicity Detection Kit. PMA-primed THP-1 cells were treated with Al_2O_3 particles of different shapes for 24 h. Data are represented as mean ± SD ($n = 5$). **c** Effects of Al_2O_3 particles of different shapes on IL-1β production were measured. PMA-primed THP-1 cells were treated with Al_2O_3 particles of different shapes for 6 h. IL-1β levels in culture supernatant were measured by ELISA. Data are represented as mean ± SD ($n = 3$). *$p < 0.001$ versus untreated control (Student's t test)

higher IL-1β production than L-Al_2O_3 (Fig. 1c). The induction of IL-1β production was observed at 100 μg/mL of N-Al_2O_3 and above. Overall IL-1β production with Al_2O_3 particles were in the order of S-Al_2O_3 > N-Al_2O_3 >> L-Al_2O_3. This result confirms the importance of investigating the relationship between inflammatory responses and biological effects of Al_2O_3 particles, especially according to particle characteristics such as size and shape.

Phagocytosis of Al_2O_3 particles

To visualize the uptake of Al_2O_3 particles in PMA-primed THP-1 cells, TEM was employed. TEM images of Fig. 2a–h show that all types of Al_2O_3 particles were taken up into the cytoplasm. Although L-Al_2O_3 particles are shaped like thin threads, they were conglomerated into a lump and appeared as a big dark spot under TEM (Fig. 2b, f). N-Al_2O_3 (Fig. 2c, g) and S-Al_2O_3 (Fig. 2d, h) both appeared as loose conglomerations in the vacuole. Phagocytosis of foreign particles by macrophages initiates the innate immune response which includes IL-1β production (Aderem and Underhill 1999). To investigate the correlation between phagocytosis of Al_2O_3 particles and IL-1β production, PMA-primed THP-1 cells were treated with different Al_2O_3 particles in the presence of cytochalasin D, a well-characterized inhibitor of phagocytosis that impairs actin filament assembly. Cytochalasin D treatment almost completely abolished IL-1β production with all shapes of Al_2O_3 particles (Fig. 2i). These results indicate that uptake of Al_2O_3 particles by phagocytosis might be the first step in the inflammatory response.

Lysosomal destabilization and cathepsin B leakage

A few research groups reported that lysosomal destabilization and the resulting release of endosomal enzymes such as cathepsin B can play important roles in the activation of NALP3 inflammasome (Hornung et al. 2008; Morishige et al. 2010). Destabilization of the lysosomal membrane after exposure to Al_2O_3 particles was evaluated by acridine orange staining using flow cytometry. Acridine orange becomes highly concentrated in acidic compartments such as lysosomes and, after membrane damage of these compartments, a decrease in red fluorescence is induced (Thibodeau et al. 2004). Acridine orange staining revealed that, in general, N- and S-Al_2O_3 particles induced more destabilization of lysosomal membranes than L-Al_2O_3 (Fig. 3a). Overall lysosomal destabilization was

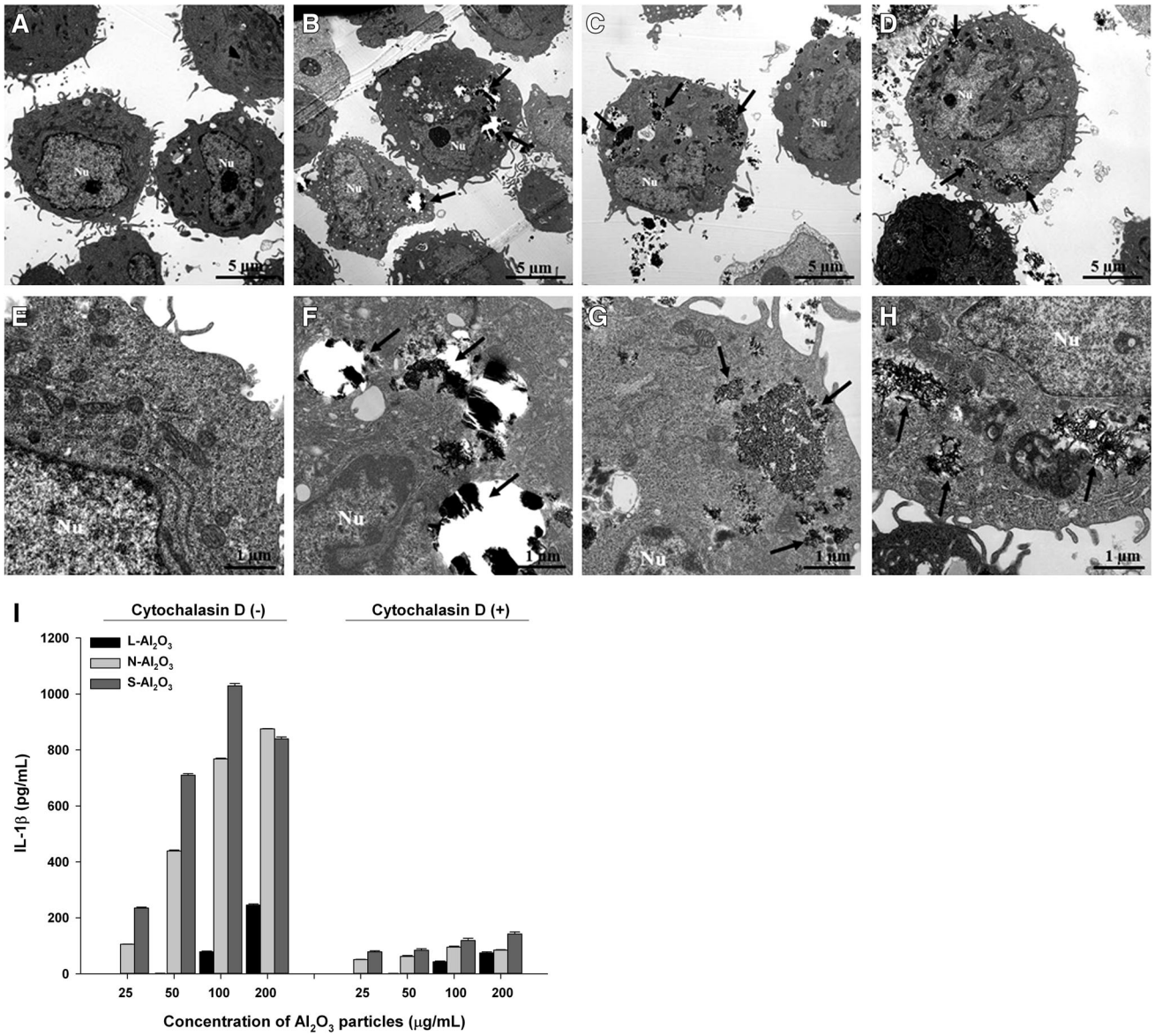

Fig. 2 Observation of particle phagocytosis into PMA-primed THP-1 cells. **a** TEM image of normal THP-1 cells without nanoparticle exposure (×6,000). TEM image of PMA-primed THP-1 cells after 6 h treatment with 50 μg/mL of **b** L-Al_2O_3, **c** N-Al_2O_3, **d** S-Al_2O_3, respectively (×6,000). Higher magnification of the TEM image is shown for **e** normal THP-1 cells, **f** L-Al_2O_3, **g** N-Al_2O_3, **h** S-Al_2O_3 (×25,000). All *arrows* indicate the presence of Al_2O_3 particles. **i** Involvement of phagocytosis in Al_2O_3-induced IL-1β production. Cells were treated with Al_2O_3 particles of different shapes for 6 h in the absence or presence of cytochalasin D (5 μM). IL-1β levels in culture supernatant were measured by ELISA. Data are represented as mean ± SD ($n = 3$)

in the order of S-Al_2O_3 > N-Al_2O_3 > L-Al_2O_3. These results suggest that phagocytosis of N- and S-Al_2O_3 particles leads to the formation of discrete vacuoles or lysosomes around particles, followed by lysosomal membrane destabilization and resulting in the release of lysosomal proteases including cathepsin B into the cytoplasm.

We speculated that Al_2O_3-induced cytotoxicity is partially dependent on the release of cathepsin B into the cytoplasm. To investigate whether the release of cathepsin B is associated with Al_2O_3-induced cytotoxicity, the cells were treated with the different kinds of Al_2O_3 particles in the presence or absence of cathepsin B-specific inhibitor CA-074-Me. The addition of CA-074-Me significantly suppressed the cytotoxicity of N- and S-Al_2O_3 as observed by the level of IL-1β production (Fig. 3b). These results indicate that Al_2O_3–induced cytotoxicity is partially associated with lysosomal destabilization, by which phagosomal contents such as cathepsin B might be released into the cytoplasm. The released cathepsin B may induce activation of caspase-1 and subsequent IL-1β production as described below.

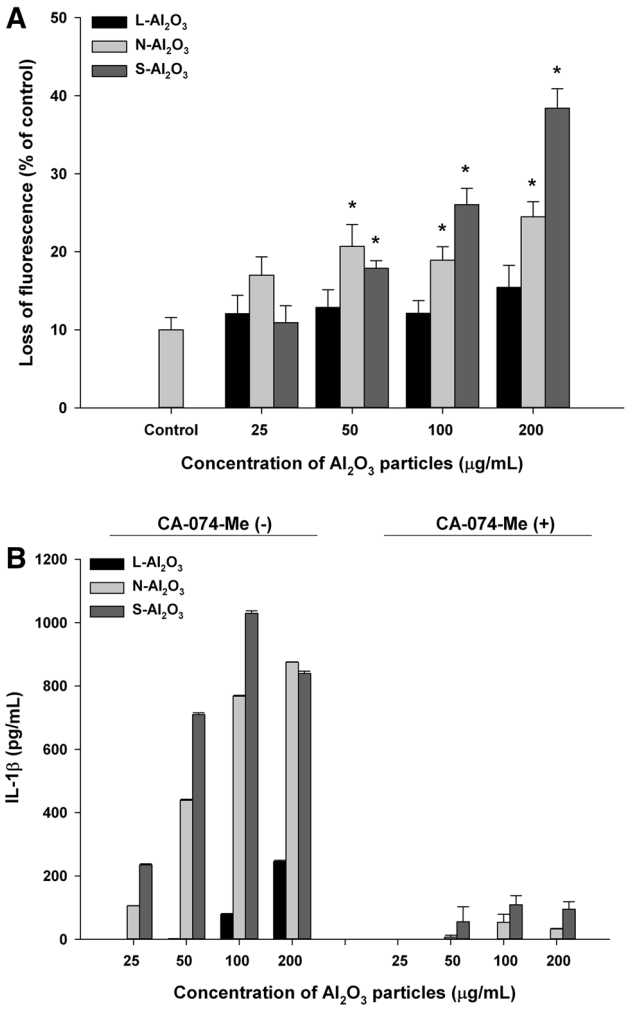

Fig. 3 Involvement of lysosomal destabilization and cathepsin B in Al_2O_3-induced IL-1β production. **a** Lysosomal destabilization as measured by fluorescence loss of Acridine orange. Data are represented as mean ± SD ($n = 3$). *$p < 0.01$ versus untreated control (Student's t test). **b** Involvement of cathepsin B in Al_2O_3-induced IL-1β production. Cells were treated with Al_2O_3 particles of different shapes for 6 h in the absence or presence of CA-074-Me, a cathepsin B-specific inhibitor (10 μM). IL-1β levels in culture supernatant were measured by ELISA. Data are represented as mean ± SD ($n = 3$)

Correlation between IL-1β production and ROS generation

Recent studies showed that the generation of ROS activates the NALP3 inflammasome (Martinon 2010; Tschopp and Schroder 2010). To investigate the correlation between ROS generation and IL-1β production in the presence of Al_2O_3 particles, ROS levels were measured in Al_2O_3-treated THP-1 cells using DCFH-DA (Fig. 4). The results showed that all shapes of Al_2O_3 particles caused an increase in the amount of intracellular ROS compared to the control (Fig. 4a). Among them, S-Al_2O_3 particles induced higher ROS generation than the other particles. Overall effects on ROS generation were in the order of S-Al_2O_3 > N-Al_2O_3 > L-Al_2O_3. To further confirm whether ROS generation is involved in Al_2O_3-induced IL-1β production, the cells were treated with the Al_2O_3 particles of different shapes in the presence of either a specific inhibitor of NADPH oxidase (DPI) or a broad ROS scavenger (BHA). NADPH oxidase is an important enzyme for the production of ROS (Morel et al. 1991). As expected, the presence of DPI and BHA both suppressed IL-1β production regardless of the shape and amount of Al_2O_3 particles (Fig. 4b). BHA was more effective in the suppression of IL-1β production than DPI. As the concentration of BHA and DPI increased, IL-1β production decreased, meaning that stronger suppression of ROS generation resulted in lower production of IL-1β (Supplementary Fig. S1). Collectively, these results indicate that phagocytosis of Al_2O_3 particles leads to the generation of intracellular ROS, which triggers IL-1β production.

Involvement of caspase-1 in Al_2O_3-induced IL-1β production

Because protease caspase-1 plays an important role in regulating the cleavage and maturation of the precursor form of IL-1β, caspase-1 is critically involved in inflammatory responses (Halle et al. 2008). Therefore, to investigate whether activation of caspase-1 is involved in Al_2O_3-induced IL-1β production, THP-1 cells were treated with different shapes and concentrations of Al_2O_3 particles in the presence of a caspase-1 specific inhibitor (Z-WEHD-FMK) and the levels of IL-1β production were analyzed. The results showed that the inhibitor suppressed Al_2O_3-induced IL-1β production according to the shape and concentration of Al_2O_3 particles (Fig. 5). These data suggest that the IL-1β release is, at least in part, mediated by activation of caspase-1.

Apoptosis and necrosis in the presence of Al_2O_3 particles

To investigate the mode of cell death induced by Al_2O_3 particles, the cells treated with Al_2O_3 particles were stained with Annexin V- FITC and PI for flow cytometric analysis. The results of Annexin V staining indicated that the degree of cell death was shape- and concentration-dependent (Fig. 6). Especially, the presence of N-Al_2O_3 and S-Al_2O_3 decreased the percentage of live cells to 56.5 and 51.7 %, respectively. There was an increase in the overall percentage of apoptotic cells with increasing concentrations of N- and S-Al_2O_3 from 25 to 100 μg/mL. The percentage of necrotic cells also increased depending on the shape and concentration of Al_2O_3 particles. At concentrations of 200 μg/mL N-Al_2O_3 and S-Al_2O_3, the percentages of necrotic cells were 27.7 and 37.5 %, respectively. The

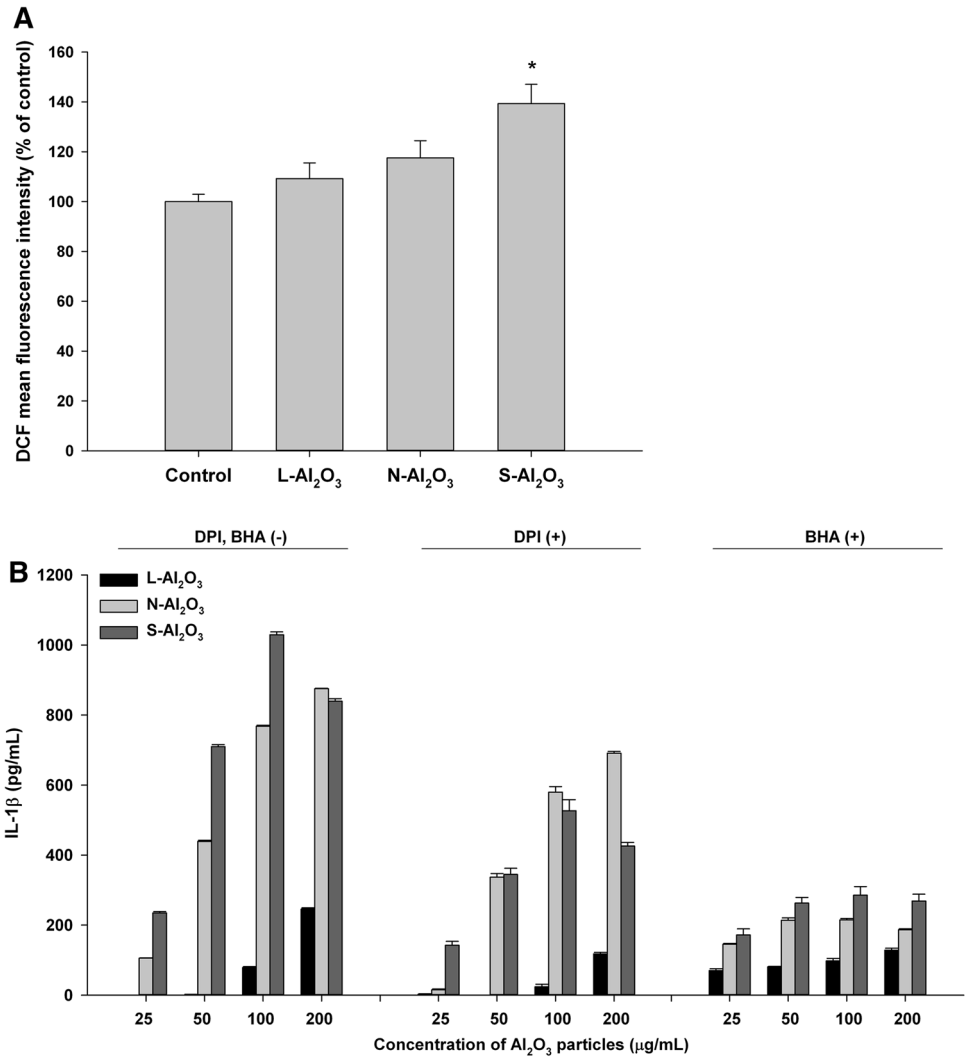

Fig. 4 Association between ROS generation and IL-1β production in the presence of Al_2O_3 particles. **a** PMA-primed THP-1 cells were treated with Al_2O_3 particles (100 μg/mL) for 24 h. At the end of exposure, the cells were loaded with DCFH-DA (20 μM) for 45 min and analyzed by flow cytometry to determine the fluorescence intensity. Data are represented as mean ± SD ($n = 3$). *$p < 0.05$ versus untreated control (Student's *t* test). **b** Cells were treated with Al_2O_3 particles of different shapes for 6 h in the absence or presence of DPI (10 μM) and BHA (100 μM). IL-1β levels in culture supernatant were measured by ELISA. Data are represented as mean ± SD ($n = 3$)

overall degree of cell death induced by Al_2O_3 particles was in the order of S-Al_2O_3 > N-Al_2O_3 > L-Al_2O_3.

Discussion

Manufactured NPs have diversified applications in many fields, so it is conceivable that they can cause harmful effects on human health and environment. Therefore, investigation of inflammatory responses and toxicity induced by these NPs is necessary. This study aimed to elucidate the mechanisms of the inflammatory effect and cytotoxicity induced by Al_2O_3 particles of different shapes. To accomplish these goals, we investigated IL-1β production as well as cytotoxicity in the presence of Al_2O_3 particles as mature IL-1βs possess potent pro-inflammatory activities which include initiation of acute phase responses and activation of lymphocytes (Dinarello 1998). We hypothesized that Al_2O_3 particles of different shapes induce different levels of inflammatory responses and cytotoxicity. Our results confirmed that Al_2O_3 particles of different shapes induce different levels of IL-1β production and cytotoxicity in THP-1 cells (Fig. 1). Based on these results, we further investigated the detailed mechanisms of IL-1β production and cytotoxicity in the presence of various shapes of Al_2O_3 particles.

First, the association between phagocytosis and IL-1β production was investigated in the presence of Al_2O_3 particles. This is because phagocytosis of foreign particles by macrophages can trigger the production of cytokines such as IL-1β as part of the immune response (Aderem and Underhill 1999). When THP-1 cells were treated with Al_2O_3 particles in the presence of cytochalasin D, IL-1β production was significantly suppressed (Fig. 2b). Furthermore, TEM analysis showed that all tested shapes of Al_2O_3 particles were taken up into the cytoplasm by THP-1

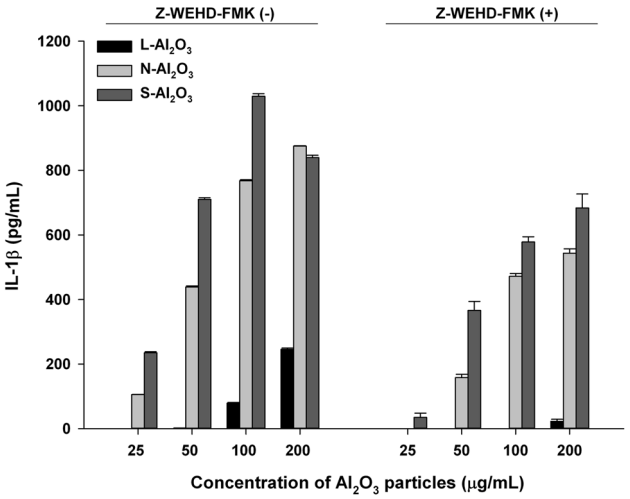

Fig. 5 Involvement of activated caspase-1 in Al_2O_3-induced IL-1β production. PMA-primed THP-1 cells were treated with Al_2O_3 particles of different shapes for 6 h in the absence or presence of Z-WEHD-FMK (10 μM). IL-1β levels in culture supernatant were measured by ELISA. Data are represented as mean ± SD ($n = 3$)

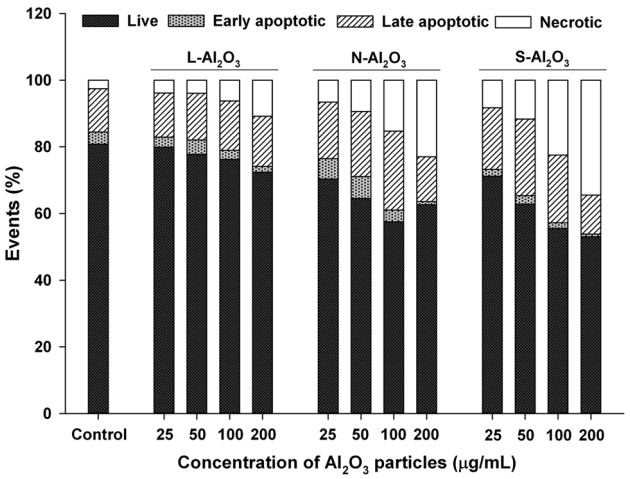

Fig. 6 Annexin V and PI staining of PMA-primed THP-1 cells to detect the mode of cell death. Cells were treated with Al_2O_3 particles of different shapes for 6 h and the percentage of apoptotic and necrotic cells was determined from quadrants of flow cytometry data

cells (Fig. 2a–h). Collectively, these results indicate that actin-filament-dependent phagocytosis is an early signal for Al_2O_3-induced IL-1β production.

Next, the mechanisms of Al_2O_3-induced IL-1β production were investigated to reveal why Al_2O_3 particles induce different levels of IL-1β production according to their shapes. A few recent studies demonstrated that phagocytosis of crystals leads to active swelling of phagolysosomes and that coincident disruption of lysosomes could lead to the release of lysosomal protease cathepsin B into the cytoplasm, which triggers activation of NAPL3 inflammasome directly or indirectly through an unknown pathway (Halle et al. 2008; Hornung et al. 2008). We observed that the degree of lysosomal destabilization was concentration-dependent and followed the general order of S-Al_2O_3 > N-Al_2O_3 > L-Al_2O_3 (Fig. 3a). The order was also observed with Al_2O_3-induced IL-1β production (Fig. 1c) and caspase-1 activation (Fig. 5). Use of CA-074-Me, a cathepsin B-specific inhibitor, effectively suppressed the IL-1β production induced by all shapes of Al_2O_3 particles (Fig. 3b). Therefore, the results suggest that phagocytosis of Al_2O_3 particles leads to significant lysosomal destabilization, followed by release of cathepsin B, which then leads to the activation of NAPL3 inflammasomes. On the other hand, the NALP3 inflammasome complex is required for the activation of procaspase-1. Once activated, protease caspase-1 regulates the cleavage and maturation of the precursor form of IL-1β (Dinarello 1998). We have shown that inhibition of caspase-1 leads to the down-regulation of IL-1β production (Fig. 5). The extent of IL-1β induction was also affected by both kinds of Al_2O_3 particles and the differential concentration of Al_2O_3 particles.

It has also been demonstrated that ROS production activates NAPL3 inflammasomes. The increase of intracellular ROS concentration results in NALP3 inflammasome activation through the dissociation of thioredoxin-interacting protein (TXNIP) from thioredoxin (Dostert et al. 2008; Zhou et al. 2010). We have shown that higher levels of intracellular ROS were generated by Al_2O_3 particles of different shapes than by the control (Fig. 4a) and that Al_2O_3-induced IL-1β production is associated with increase of intracellular ROS (Fig. 4b). These results indicated that not only cathepsin B released from the lysosome but also ROS generated by Al_2O_3 particles play crucial roles in Al_2O_3-induced IL-1β production, possibly interacting with each other in the process. We also believe that the Al_2O_3 particles are phagocytosized first. The reactive surface of Al_2O_3 particles may then interact with phagolysosomal membranes while producing ROS, leading to at least partial lysosomal rupture. As evidenced by the higher LDH values, N-Al_2O_3 (sphere shape, <50 nm; nominal surface area <7,853 nm^2) and S-Al_2O_3 (short thread shape, 2–4 nm × 100–800 nm; aspect ratio of 25–400; nominal surface area = 635–10,078 nm^2) caused more membrane damage and more ROS production than L-Al_2O_3 (long thread shape, 2–4 nm × 2,800 nm; aspect ratio of 700–1,400; nominal surface area = 17,599–35,210 nm^2). It is well known that round shaped NPs are more toxic than round shaped microparticles (MPs) due to the larger surface area (Hsiao and Huang 2011; Jung et al. 2014; Lee et al. 2014). However, there have been a limited number of studies comparing cytotoxicity between round shaped NPs and thread (or rod) shaped MPs. The data above shows that thread-shaped MPs can be more cytotoxic than round-shaped NPs, depending on aspect ratio. Many

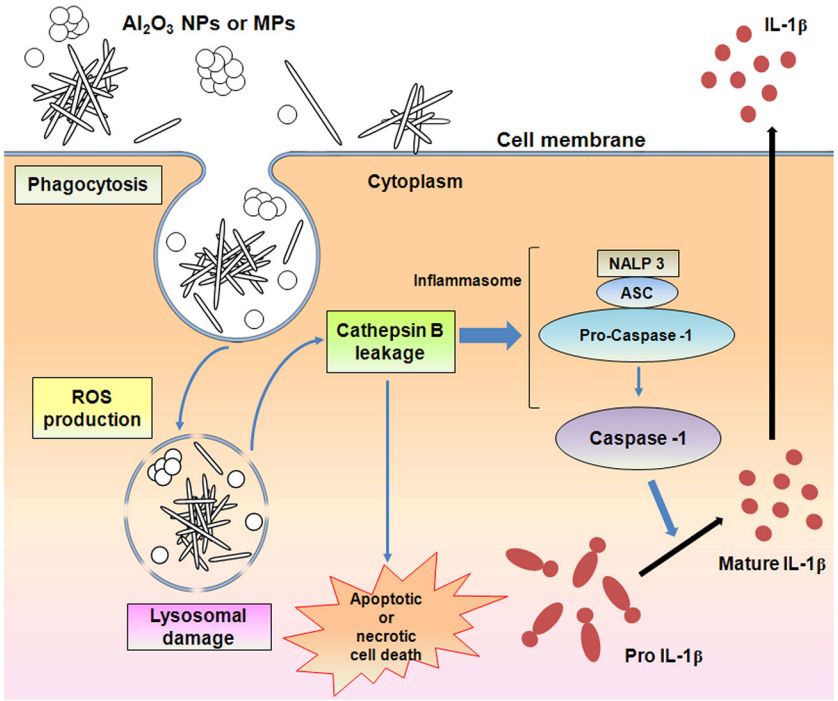

Fig. 7 Proposed mechanism for IL-1β production and cytotoxicity by Al_2O_3 particles in PMA-primed THP-1 cells. It is proposed that IL-1β production induced by Al_2O_3 particles is mediated by phagocytosis, generation of ROS, lysosomal damage, cathepsin B leakage, and activation of caspase-1 by NALP3 inflammasome. Cell death by Al_2O_3 particles may involve a cathepsin B-dependent pathway

previous studies showed that the surface area of particles is a critical factor influencing cytotoxicity (Hsiao and Huang 2011; Jung et al. 2014; Lee et al. 2014). Our results show that aspect ratio as well as surface area needs to be considered when evaluating cytotoxicity caused by thread-like MPs. In the present study, we found that MPs with higher aspect ratios are much less cytotoxic than round-shaped NPs or MPs with lower aspect ratios.

The cytotoxicity of Al_2O_3 particles was investigated using PMA-primed THP-1 cells with WST-1 assay. The degree of cytotoxicity was in the order of S-Al_2O_3 > N-Al_2O_3 > L-Al_2O_3 (Fig. 1a). Fujisawa et al. (2007) demonstrated that lysosomal destabilization leads to the release of lysosomal protease, especially cathepsin B, and subsequent rapid cell death via a variety of stimuli. We also found that Al_2O_3-induced cell death as measured by WST-1 assay was significantly suppressed by the presence of CA-074-Me (Supplementary Fig. S2), indicating that the cell death induced by Al_2O_3 particles may involve a cathepsin B-dependent pathway. Annexin V and PI staining showed that both N- and S-Al_2O_3 significantly increased the percentages of necrotic cells (Fig. 6). Collectively, these results imply that as the concentration of Al_2O_3 particles increases, the mode of cell death is more likely to become necrotic rather than late apoptotic.

In conclusion, all results of the present study show that Al_2O_3 particles induce different levels of IL-1β production and cytotoxicity depending on their particle shapes or aspect ratios and that the lysosomal destabilization and subsequent release of cathepsin B act as an important upstream signal in the IL-1β production pathway induced by Al_2O_3 particles. Furthermore, it was confirmed that the generation of intracellular ROS caused by Al_2O_3 particles varied according to their shapes and aspect ratios, and triggered Al_2O_3-induced IL-1β production and apoptosis (or necrosis). Based on these results, we propose a mechanism for IL-1β production and cytotoxicity (Fig. 7). Thus, our findings might support an ideal foundation for development of safe shapes of Al_2O_3 particles.

Acknowledgments This work was supported by a Grant from the National Research Foundation of Korea (NRF-2011-0017012) and a Korea University Grant.

References

Aderem A, Underhill DM (1999) Mechanisms of phagocytosis in macrophages. Annu Rev Immunol 17:593–623

Agostini L, Martinon F, Burns K, McDermott MF, Hawkins PN, Tschopp J (2004) NALP3 forms an IL-1β-processing inflammasome with increased activity in Muckle-Wells autoinflammatory disorder. Immunity 20:319–325

Allen IC, Scull MA, Moore CB, Holl EK, McElvania-TeKippe E, Taxman DJ, Guthrie EH, Pickles RJ, Ting JPY (2009) The NLRP3 inflammasome mediates in vivo innate immunity to influenza A virus through recognition of viral RNA. Immunity 30:556–565

Arrigo AP, Firdaus WJJ, Mellier G, Moulin M, Paul C, Diaz-latoud C, Kretz-remy C (2005) Cytotoxic effects induced by oxidative stress in cultured mammalian cells and protection provided by Hsp27 expression. Methods 35:126–138

Boya P, Andreau K, Poncet D, Zamzami N, Perfettini JL, Metivier D, Ojcius DM, Jaattela M, Kroemer G (2003) Lysosomal membrane permeabilization induces cell death in a mitochondrion-dependent fashion. J Exp Med 197:1323–1334

Burns K, Martinon F, Tschopp J (2003) New insights into the mechanism of IL-1β maturation. Curr Opin Immunol 15:26–30

Dinarello CA (1998) Interleukin-1β, interleukin-18, and the interleukin-1β converting enzyme. Ann N Y Acad Sci 856:1–11

Dostert C, Pétrilli V, Van Bruggen R, Steele C, Mossman BT, Tschopp J (2008) Innate immune activation through Nalp3 inflammasome sensing of asbestos and silica. Science 320:674–677

Fujisawa A, Kambe N, Saito M, Nishikomori R, Tanizaki H, Kanazawa N, Adachi S, Heike T, Sagara J, Suda T (2007) Disease-associated mutations in CIAS1 induce cathepsin B-dependent rapid cell death of human THP-1 monocytic cells. Blood 109:2903–2911

Halle A, Hornung V, Petzold GC, Stewart CR, Monks BG, Reinheckel T, Fitzgerald KA, Latz E, Moore KJ, Golenbock DT (2008) The NALP3 inflammasome is involved in the innate immune response to amyloid-β. Nat Immunol 9:857–865

Hiura TS, Kaszubowski MP, Li N, Nel AE (1999) Chemicals in diesel exhaust particles generate reactive oxygen radicals and induce apoptosis in macrophages. J Immunol 163:5582–5591

Hornung V, Bauernfeind F, Halle A, Samstad EO, Kono H, Rock KL, Fitzgerald KA, Latz E (2008) Silica crystals and aluminum salts activate the NALP3 inflammasome through phagosomal destabilization. Nat Immunol 9:847–856

Hsiao IL, Huang YJ (2011) Effects of various physicochemical characteristics on the toxicities of ZnO and TiO2 nanoparticles toward human lung epithelial cells. Sci Total Environ 409:1219–1228

Jung HJ, Pak PJ, Park SH, Ju JE, Kim JS, Lee HS, Chung N (2014) Silver wire amplifies the signaling mechanism for IL-1β production more than silver submicroparticles in human monocytic THP-1 cells. Plos One 9:e112256. doi:10.1371/journal.pone.0112256

Kim YJ, Choi HS, Song MK, Youk DY, Kim JH, Ryu JC (2009) Genotoxicity of aluminum oxide (Al_2O_3) nanoparticle in mammalian cell lines. Mol Cell Toxicol 5:172–178

Lee JH, Ju JE, Kim BI, Pak PJ, Choi EK, Lee HS, Chung N (2014) Rod-shaped iron oxide nanoparticle is more toxic differentially than round-shaped iron oxide nanoparticle. Environ Toxicol Chem 33:2759–2766

Li Y, Yang XY, Feng Y, Yuan ZY, Su BL (2012) One-dimensional metal oxide nanotubes, nanowires, nanoribbons, and nanorods: synthesis, characterizations, properties and applications. Crit Rev Solid State 37:1–74

Martinon F (2010) Signaling by ROS drives inflammasome activation. Eur J Immunol 40:616–619

Morel F, Doussiere J, Vignais PV (1991) The superoxide generating oxidase of phagocytic cells. Eur J Biochem 201:523–546

Morishige T, Yoshioka Y, Inakura H, Tanabe A, Yao X, Narimatsu S, Monobe Y, Imazawa T, Tsunoda S, Tsutsumi Y (2010) The effect of surface modification of amorphous silica particles on NLRP3 inflammasome mediated IL-1β production, ROS production and endosomal rupture. Biomaterials 31:6833–6842

Morsy GM, Abou El-Ala KS, Ali AA (2013) Studies on fate and toxicity of nanoalumina in male albino rats: lethality, bioaccumulation and genotoxicity. Toxicol Ind Health. doi:10.1177/0748233713498449

Piccinno F, Gottschalk F, Seeger S, Nowack B (2012) Industrial production quantities and uses of ten engineered nanomaterials in Europe and the world. J Nanoparticle Res 14:1109

Roy CJ, Chorine N, De Geest BG, De Smedt S, Jonas AM, Demoustier-Champagne S (2012) Highly versatile approach for preparing functional hybrid multisegmented nanotubes and nanowires. Chem Mater 24:1562–1567

Stutz A, Golenbock DT, Latz E (2009) Inflammasomes: too big to miss. J Clin Investig 119:3502–3511

Thibodeau MS, Giardina C, Knecht DA, Helble J, Hubbard AK (2004) Silica-induced apoptosis in mouse alveolar macrophages is initiated by lysosomal enzyme activity. Toxicol Sci 80:34–48

Tschopp J, Schroder K (2010) NLRP3 inflammasome activation: the convergence of multiple signaling pathways on ROS production? Nat Rev Immunol 10:210–215

Yagil-Kelmer E, Kazmier P, Rahaman MN, Bal BS, Tessman RK, Estes DM (2004) Comparison of the response of primary human blood monocytes and the U937 human monocytic cell line to two different sizes of alumina ceramic particles. J Orthop Res 22:832–838

Zhou R, Tardivel A, Thorens B, Choi I, Tschopp J (2010) Thioredoxin-interacting protein links oxidative stress to inflammasome activation. Nat Immunol 11:136–140